LETTERS

Following the signal sequence from ribosomal tunnel exit to signal recognition particle

Mario Halic[1]*, Michael Blau[1]*, Thomas Becker[1], Thorsten Mielke[2], Martin R. Pool[3], Klemens Wild[4], Irmgard Sinning[4] & Roland Beckmann[1,2]

Membrane and secretory proteins can be co-translationally inserted into or translocated across the membrane[1]. This process is dependent on signal sequence recognition on the ribosome by the signal recognition particle (SRP), which results in targeting of the ribosome–nascent-chain complex to the protein-conducting channel at the membrane[2,3]. Here we present an ensemble of structures at subnanometre resolution, revealing the signal sequence both at the ribosomal tunnel exit and in the bacterial and eukaryotic ribosome–SRP complexes. Molecular details of signal sequence interaction in both prokaryotic and eukaryotic complexes were obtained by fitting high-resolution molecular models. The signal sequence is presented at the ribosomal tunnel exit in an exposed position ready for accommodation in the hydrophobic groove of the rearranged SRP54 M domain. Upon ribosome binding, the SRP54 NG domain also undergoes a conformational rearrangement, priming it for the subsequent docking reaction with the NG domain of the SRP receptor. These findings provide the structural basis for improving our understanding of the early steps of co-translational protein sorting.

Elongation-arrested *Escherichia coli* 70S ribosomes were purified from an *in vitro* translation system[4]. As a nascent chain we used the first 102 amino acid residues of the membrane protein FtsQ, which contain a single transmembrane segment serving as an SRP-dependent signal sequence[5]. Purified 70S ribosome–nascent-chain complexes (RNCs) were reconstituted with recombinant SRP and subjected to structure determination by cryo-electron microscopy and single-particle analysis. To reach subnanometre resolution, sorting of the data sets[6] was necessary.

The structure of a 70S RNC carrying a signal sequence was reconstructed at 9.1 Å resolution from particles that were combined after sorting on the basis of the presence of P-site tRNA and the absence of a ligand. The reconstruction showed the expected P-site peptidyl-tRNA and, in addition, an elongated density located directly at the ribosomal tunnel exit site (Fig. 1a, b). This density is not present in comparable reconstructions at 9 Å resolution[7] such as that of a stalled *E. coli* 70S ribosome without a nascent chain (Fig. 1c). Because extended peptide chains would hardly be resolved at the present resolution, this density most probably represents the signal sequence of FtsQ in an α-helical conformation, which it might already have adopted in the ribosomal tunnel[8,9]. The density is in contact with a protruding hairpin structure of ribosomal protein L24p. It is also in the immediate vicinity of the rRNA helices 59 and 24, and the proteins L23p and L29p (Fig. 1d), which is in excellent agreement with chemical crosslinks between FtsQ and L23p (ref. 5). Because the density did not show the clear rod-like shape as observed for α-helices in several ribosomal proteins of this reconstruction, it is likely that

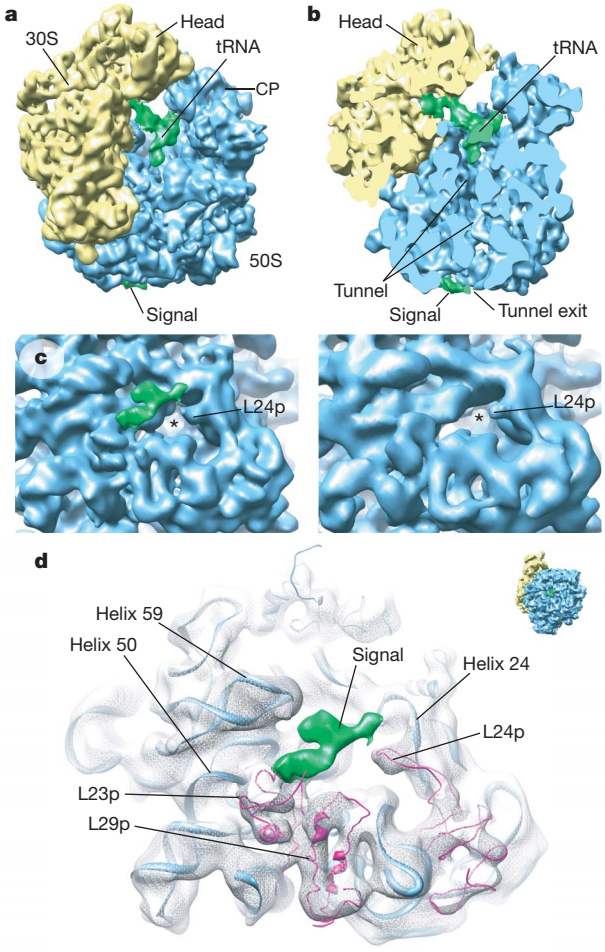

Figure 1 | Cryo-electron microscopic structure of programmed 70S ribosome (RNC) with signal sequence. **a**, Density map with the ribosomal 30S subunit shown in yellow, 50S in blue and the P-site tRNA and nascent chain (signal sequence) in green. Landmarks are indicated. CP, central protuberance. **b**, Section through the ribosome showing the signal sequence at the tunnel exit site. **c**, Comparison of the ribosomal tunnel exit site of 70S RNC (left) with the empty 70S ribosome (3D-EM database accession number EMD1055)[7] (right). Additional density (signal sequence) is shown in green. **d**, View as in **c**, with ribosomal density shown as a white mesh and models as ribbons. rRNA is shown in blue; L23p, L24p and L29p in magenta; signal sequence in green.

[1]Gene Center, Department of Chemistry and Biochemistry, University of Munich, Feodor-Lynen-Strasse 25, 81377 Munich, Germany. [2]UltraStructureNetwork, USN, Max Planck Institute for Molecular Genetics, Ihnestrasse 63–73, 14195 Berlin, Germany. [3]Faculty of Life Sciences, Michael Smith Building, University of Manchester, Oxford Road, Manchester M13 9PT, UK. [4]Heidelberg University Biochemistry Center (BZH), Im Neuenheimer Feld 328, D-69120 Heidelberg, Germany.
*These authors contributed equally to this work.

the signal sequence confers some flexibility at this site. Targeting factors or chaperones can easily interact with the signal sequence in its exposed position. Because SRP can interact with signal sequences in nascent chains of various lengths[10,11], the observed site could serve as a parking position at the tunnel exit where signal sequences are retained for recognition by SRP[12].

The reconstruction of the *E. coli* 70S RNC–SRP complex at 9.4 Å revealed a large density at the tunnel exit representing SRP (Fig. 2a–c). As a result of conformational heterogeneity and imperfect occupancy, the local resolution of the SRP is somewhat lower than that of the ribosome (9.5–12 Å). The elongated portion showed a helical twist, with the major and minor groove representing 4.5S RNA of SRP. Attached to it is the SRP54 (Ffh in *E. coli*) by means of its well-resolved M domain[13] and, barely visible at subnanometre resolution, the SRP54 NG domain. It seems to have some freedom to move and is clearly visible only after the application of a low-pass filter, reducing the information to about 13 Å (Fig. 2b). We docked available high-resolution X-ray data[13,14] into the density and flexibly adjusted minor parts to build a molecular model of ribosome-bound *E. coli* SRP. Although the RNA of the X-ray data is truncated at loop C, we can follow it until loop E. Notably, the visible part of the 4.5S RNA has a kink of about 30° formed by the helix around nucleotide 72 next to loop C (Fig. 2c, f). Some flexibility may be provided by loop C in the RNA, and total loss of density after loop E indicates that the latter serves as a very flexible hinge[15]. Although *E. coli* SRP is positioned a few ångströms closer to the ribosome than is the mammalian SRP,

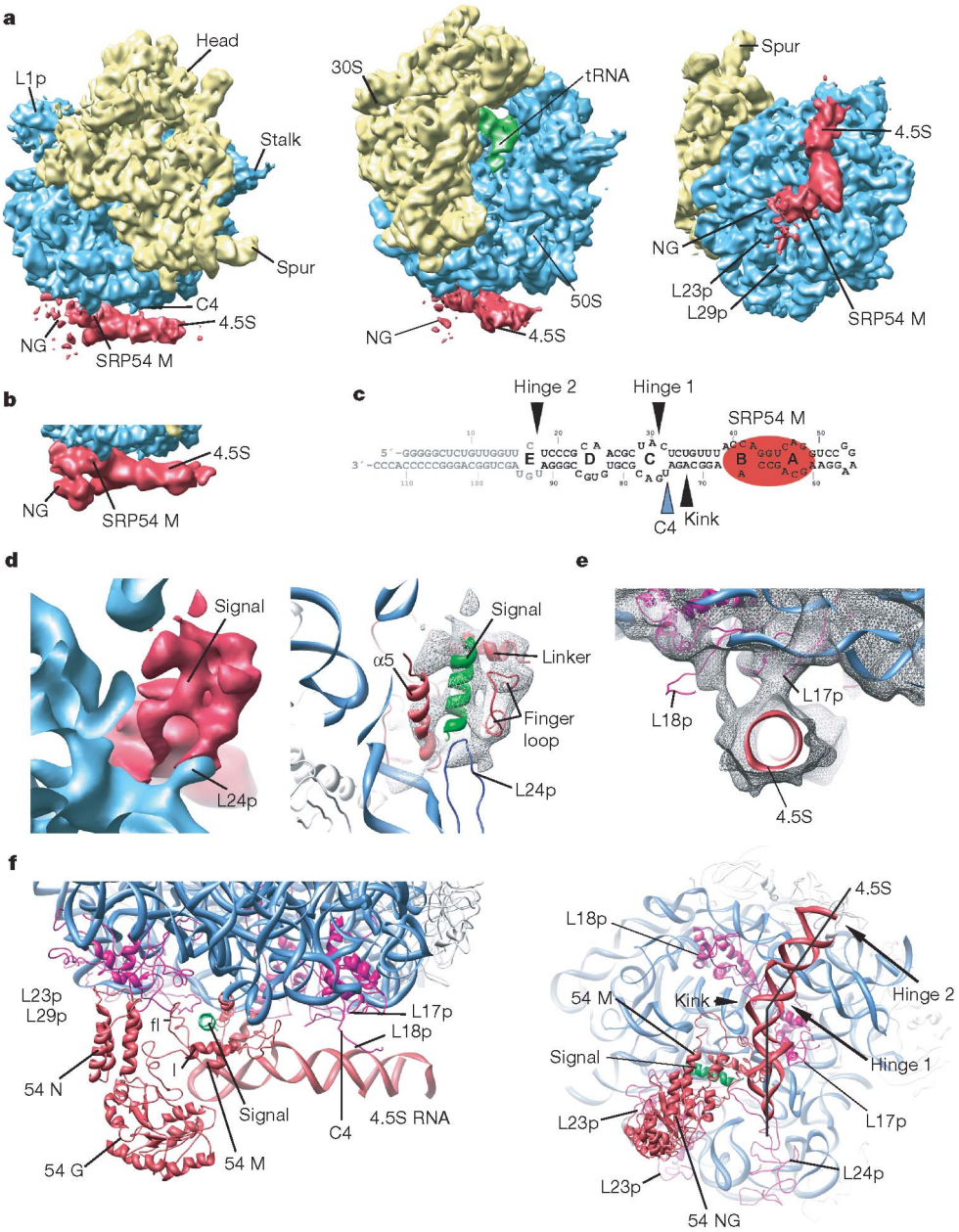

Figure 2 | Structure of *E. coli* 70S RNC–SRP complex. **a**, Density map with colour code as in Fig. 1 and SRP shown in red. Left, view onto the back of the 30S subunit; middle, side view; right, bottom view. Landmarks are indicated. **b**, SRP density filtered at a lower resolution (13 Å) and shown at a lower contour level. Note the visible NG domain. **c**, Secondary structure of *E. coli* 4.5S RNA. Red, binding region of the SRP54 M domain; grey, flexible part of SRP RNA not visible in the cryo-electron microscopic density. Arrowheads indicate hinges, kinks and interaction sites. **d**, Hydrophobic groove of the SRP54 M domain with signal sequence bound (left), and the model of SRP54 M domain (red) and the signal sequence (green) docked into the density (right). rRNA is shown in blue, L24p in dark blue. **e**, Connection 4 of *E. coli* SRP. **f**, Left, side view of the SRP-RNC model; right, bottom view.

the connections of *E. coli* SRP with the 70S ribosome are very similar to those found for the mammalian S domain[4,16]. The SRP54 NG domain interacts through the N domain with the L23p/L29p adaptor site, and the SRP54 M domain interacts with ribosomal RNA helices 24, 59 and 50. As in the eukaryotic system, the M domain might also interact with L22p (rpL17 in yeast). An entirely new contact is established between L24p and the finger loop of the SRP54 M domain (Fig. 2d), resembling the L24p contact between ribosome and TF[17]. In a similar manner to connection 4 of mammalian SRP, the SRP RNA forms a contact around nucleotide 75 in loop C of the 4.5S RNA with positively charged residues of the ribosomal protein L18p and probably also with the carboxy terminus of L17p (Fig. 2b, e). We also observed density for the linker helix connecting the M domain with the NG domain of SRP54. It is in contact with α-helix 1 and the finger loop of the SRP54 M domain as well as with the NG domain, thus efficiently coupling the signal-sequence-binding domain with the GTPase domain of SRP54 as described[18].

Notably, additional density is present in the hydrophobic groove of the SRP54 M domain (Fig. 2d), which has previously been suggested as the main signal-sequence-binding site of SRP[19]. This density, thus very probably representing the signal sequence, was observed in a position that in unbound SRP is occupied by a part of the finger loop of the SRP54 M domain. This may serve as a pseudo-substrate in the absence of a signal sequence. Because we observed only weak density for the rearranged finger loop in the RNC–SRP complex, we concluded that it does not rearrange into a distinct conformation after being pushed out of the hydrophobic groove. Although the density for the signal sequence is not reaching down to the backbone of the SRP RNA, because of possible flexibility we cannot exclude an interaction with RNA[13].

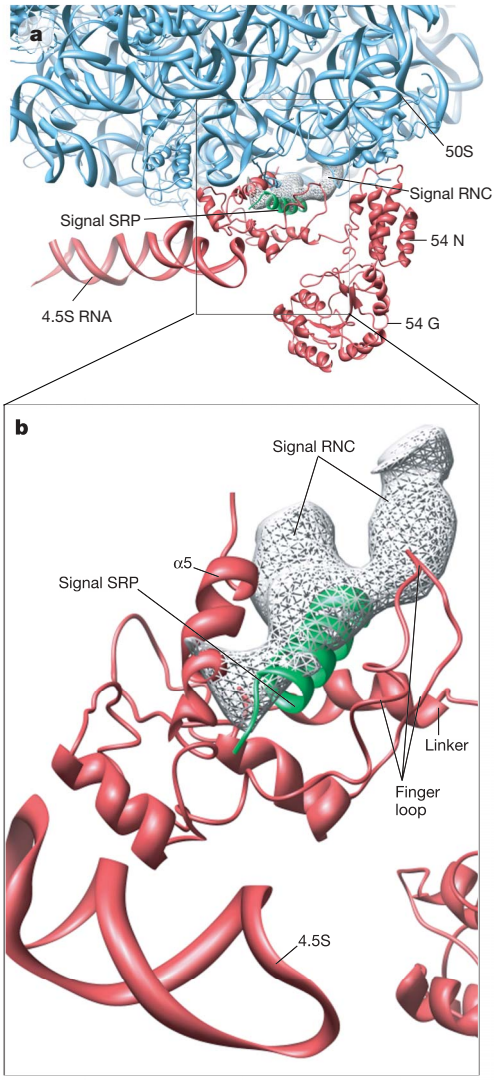

Figure 3 | Transfer of signal sequence from the ribosome to SRP. a, The models of the ribosome, SRP and the SRP-bound signal sequence are shown in blue, red and green, respectively. The density of the signal sequence bound to the ribosome (Fig. 1) is shown as a white mesh. **b**, Close-up of **a**. Note the small difference and partial overlap of the positions of the signal sequence.

The position of the signal sequence in the RNC–SRP complex is very similar to that of the ligand-free RNC-bound signal sequence (Fig. 3). Only its contact with L23p was lost in the RNC–SRP reconstruction, explaining the loss of crosslinks between L23p and the FtsQ signal sequence after SRP binding[5]. The interaction of SRP with the ribosomal adaptor site L23p/L29p may trigger the dissociation of the signal sequence and, concomitantly, the interaction of L24p with the finger loop of the SRP54 M domain may contribute to the opening of the hydrophobic groove so that the signal sequence can glide into it (Fig. 2d). However, for switching from the ribosome-bound state to the SRP-bound state the signal sequence has to move very little: SRP54 is merely locking it in by providing a matching hydrophobic environment directly at its exposed position at the tunnel exit.

We improved the cryo-electron microscopic structure of the 80S RNC in complex with the mammalian SRP[4] to a resolution of 8.7 Å (Fig. 4a). Although the local resolution of the SRP S domain is estimated to be in the range 9.5–11.5 Å, the density permitted the fitting of a molecular model for SRP54 based on α-helical secondary structure. In a very similar manner to the 70S RNC–SRP complex, docking of the M domain of mammalian SRP54 revealed additional density in the hydrophobic groove, representing the bound signal sequence (Fig. 4b, c). In comparison with the M domain in unbound SRP, the engaged M domain is rearranged when accommodating the signal sequence: the α-helix 1 is rotated upwards while still keeping the contact to the repositioned linker helix, which might involve the 'greasy slide' proposed earlier[14]. In this way the groove is formed by α-helices 1, 2 and 5, the finger loop and the linker helix. Contacts were also established between the linker helix and the finger loop, and between the G domain and α-helix 2 of the M domain. These contacts may contribute to the communication between the M and G domains of SRP54.

In comparison with the bacterial SRP54 subunit, the mammalian protein has a C-terminal extension of the M domain of about 70 amino acids, which is predicted to adopt a primarily α-helical secondary structure. Using protein threading we created a molecular model of this C terminus that could be fitted into the remaining density with only very minor modifications (Fig. 4d). It wraps around the ribosomal rRNA helix 59 and reaches up towards the tunnel exit, also interacting with ribosomal rRNA helix 50. In this position the C terminus confines the hydrophobic groove on one side and is very likely to contribute to the interaction of the SRP54 M domain with the signal sequence.

The overall geometry of the refitted SRP54 N domain[14], in particular α-helices 2 and 4, properly filled the density, but with α-helices 1 and 3 partly shifted outside (Fig. 4e, f). When using the N domain of SRP54 NG involved in the twin structure with the NG domain of the SRP receptor[20,21], it became evident that here α-helix 3 fits better, but α-helix 1 is delocalized and α-helix 4 no longer fits as a result of a rotation. This indicates that the N domain of SRP undergoes a conformational switch upon ribosome interaction, which leads to an arrangement of α-helices 2 and 3 very similar to the conformation observed in the NG twin structure. These two helices and their connecting loop include the highly conserved 'ALLEADV' motif that is involved in the interface between the two NG domains in the NG twin[20,21]. Thus, high-affinity ribosome binding seems to prime this part of the NG domain for the subsequent interaction with the SRP receptor. The reorientation of α-helices 1 and 4 of the SRP54 N domain after NG twin formation may explain how the interaction

with the SRP receptor triggers dissociation of the SRP54 NG domain from its ribosomal binding site[22].

Moreover, when adjusting the angle between the N and G domains of SRP54 we observed that the angle is very similar to that observed in the NG twin structure (Fig. 4g). Rearrangement from the monomeric to the NG twin conformation requires a rotation of about 30°; a rotation of about 25° already takes place when switching to the ribosome-bound conformation, which may also contribute to the regulation of the affinity for GTP. The entire conformation of the SRP54 NG domain is therefore rearranged on the ribosome such that it is primed for the interaction with the NG domain of the SRP receptor.

Although the resolution of the NG domain is not as good, these observations are consistent with the structure of the bacterial system. When the 70S RNC-bound SRP and the 80S RNC-bound SRP are superimposed (Fig. 4h, i), it is evident that these systems are extremely similar in their overall conformation. This indicates a high degree of structural and functional conservation, which is underlined by the fact that *in vitro* the mammalian targeting system can be functionally replaced by the bacterial one[23].

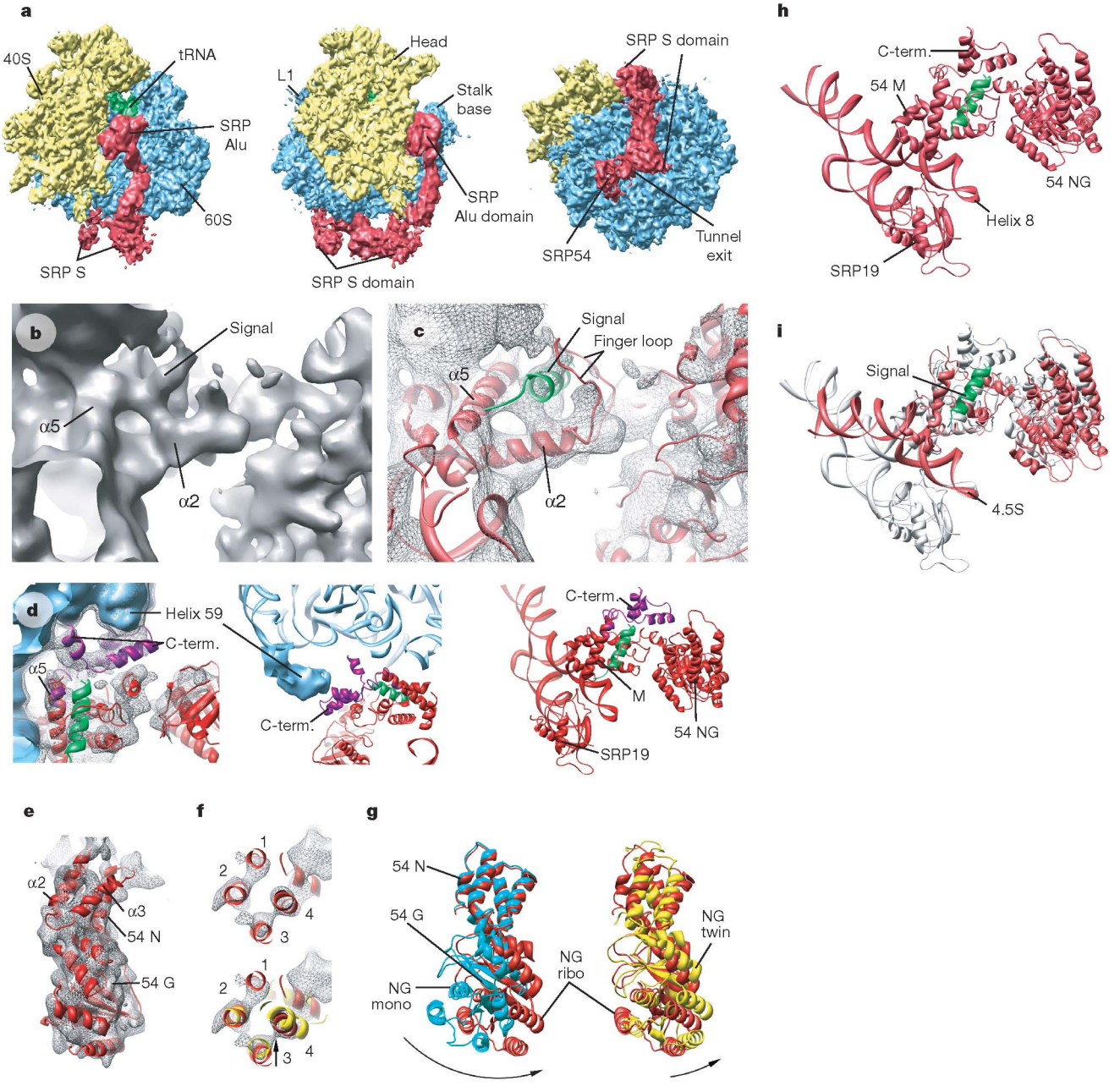

Figure 4 | Mammalian SRP bound to 80S RNC. **a**, Cryo-electron microscopic structure of the mammalian SRP bound to 80S wheat germ RNC. **b**, Density representing the hydrophobic groove of the SRP54 M domain with the signal sequence bound. **c**, Same view as in **b** showing the docked crystal structure of SRP54 M domain (red) and the signal sequence (green) docked into extra density. **d**, A model of the C-terminal part of SRP54 M domain is shown in purple docked into the additional density of SRP54 (left). SRP54 density is shown as a grey mesh, and the ribosome is shown in blue. **e**, Model of the fitted ribosome-bound mammalian NG domain. **f**, Top view of the four-helix bundle of the SRP54 N domain based on the monomeric NG domain in red (top), and superimposed on the N domain from the NG twin structure in yellow (bottom). **g**, Comparison of the model of ribosome-bound NG domain (red, NG ribo) with the monomeric unbound domain (blue, NG mono) and with the twin NG domain (yellow, NG twin). **h**, The complete model of mammalian SRP S domain (red). **i**, The *E. coli* model (red) superimposed on the mammalian model (white).

METHODS

E. coli 70S RNCs were purified and reconstituted essentially as described previously[4], with some modifications (see Supplementary Information). Samples were applied to carbon-coated holey grids[24] and micrographs were recorded on a Tecnai F30 microscope at 300 kV. The data were processed with SPIDER[25] and classified[6]. As a result, data sets of stalled ribosomes with a peptidyl-tRNA in the P-site were further split in a manner that was dependent on the presence of ligands or distinguishable conformations. The crystal structure of *E. coli* 50S subunit (Protein Data Bank (PDB) accession number 2AW4)[26] was docked with the use of Situs[27]. The *E. coli* SRP (1DUL)[13], *S. sulfataricus* SRP (1QZW)[14] and mammalian SRP structure were docked with the use of O[28], and the flexible amino-terminal part of the M domain was adjusted accordingly. Figures were prepared with Chimera[29].

Received 24 July; accepted 10 October 2006.
Published online 29 October 2006.

1. Luirink, J., von Heijne, G., Houben, E. & de Gier, J. W. Biogenesis of inner membrane proteins in *Escherichia coli*. *Annu. Rev. Microbiol.* **59,** 329–355 (2005).
2. Luirink, J. & Sinning, I. SRP-mediated protein targeting: structure and function revisited. *Biochim. Biophys. Acta* **1694,** 17–35 (2004).
3. Halic, M. & Beckmann, R. The signal recognition particle and its interactions during protein targeting. *Curr. Opin. Struct. Biol.* **15,** 116–125 (2005).
4. Halic, M. *et al.* Structure of the signal recognition particle interacting with the elongation-arrested ribosome. *Nature* **427,** 808–814 (2004).
5. Ullers, R. S. *et al.* Interplay of signal recognition particle and trigger factor at L23 near the nascent chain exit site on the *Escherichia coli* ribosome. *J. Cell Biol.* **161,** 679–684 (2003).
6. Penczek, P. A., Frank, J. & Spahn, C. M. A method of focused classification, based on the bootstrap 3D variance analysis, and its application to EF-G-dependent translocation. *J. Struct. Biol.* **154,** 184–194 (2006).
7. Valle, M. *et al.* Incorporation of aminoacyl-tRNA into the ribosome as seen by cryo-electron microscopy. *Nature Struct. Biol.* **10,** 899–906 (2003).
8. Woolhead, C. A., McCormick, P. J. & Johnson, A. E. Nascent membrane and secretory proteins differ in FRET-detected folding far inside the ribosome and in their exposure to ribosomal proteins. *Cell* **116,** 725–736 (2004).
9. Lu, J. & Deutsch, C. Secondary structure formation of a transmembrane segment in Kv channels. *Biochemistry* **44,** 8230–8243 (2005).
10. Houben, E. N., Zarivach, R., Oudega, B. & Luirink, J. Early encounters of a nascent membrane protein: specificity and timing of contacts inside and outside the ribosome. *J. Cell Biol.* **170,** 27–35 (2005).
11. Flanagan, J. J. *et al.* Signal recognition particle binds to ribosome-bound signal sequences with fluorescence-detected subnanomolar affinity that does not diminish as the nascent chain lengthens. *J. Biol. Chem.* **278,** 18628–18637 (2003).
12. Eisner, G., Moser, M., Schafer, U., Beck, K. & Muller, M. Alternate recruitment of signal recognition particle and trigger factor to the signal sequence of a growing nascent polypeptide. *J. Biol. Chem.* **281,** 7172–7179 (2006).
13. Batey, R. T., Rambo, R. P., Lucast, L., Rha, B. & Doudna, J. A. Crystal structure of the ribonucleoprotein core of the signal recognition particle. *Science* **287,** 1232–1239 (2000).
14. Rosendal, K. R., Wild, K., Montoya, G. & Sinning, I. Crystal structure of the complete core of archaeal signal recognition particle and implications for interdomain communication. *Proc. Natl Acad. Sci. USA* **100,** 14701–14706 (2003).
15. Buskiewicz, I. *et al.* Conformations of the signal recognition particle protein Ffh from *Escherichia coli* as determined by FRET. *J. Mol. Biol.* **351,** 417–430 (2005).
16. Pool, M. R., Stumm, J., Fulga, T. A., Sinning, I. & Dobberstein, B. Distinct modes of signal recognition particle interaction with the ribosome. *Science* **297,** 1345–1348 (2002).
17. Schlunzen, F. *et al.* The binding mode of the trigger factor on the ribosome: implications for protein folding and SRP interaction. *Structure* **13,** 1685–1694 (2005).
18. Wild, K., Halic, M., Sinning, I. & Beckmann, R. SRP meets the ribosome. *Nature Struct. Mol. Biol.* **11,** 1049–1053 (2004).
19. Bernstein, H. D. *et al.* Model for signal sequence recognition from amino-acid sequence of 54K subunit of signal recognition particle. *Nature* **340,** 482–486 (1989).
20. Egea, P. F. *et al.* Substrate twinning activates the signal recognition particle and its receptor. *Nature* **427,** 215–221 (2004).
21. Focia, P. J., Shepotinovskaya, I. V., Seidler, J. A. & Freymann, D. M. Heterodimeric GTPase core of the SRP targeting complex. *Science* **303,** 373–377 (2004).
22. Halic, M. *et al.* Signal recognition particle receptor exposes the ribosomal translocon binding site. *Science* **312,** 745–747 (2006).
23. Powers, T. & Walter, P. Co-translational protein targeting catalyzed by the *Escherichia coli* signal recognition particle and its receptor. *EMBO J.* **16,** 4880–4886 (1997).
24. Wagenknecht, T., Grassucci, R. & Frank, J. Electron microscopy and computer image averaging of ice-embedded large ribosomal subunits from *Escherichia coli*. *J. Mol. Biol.* **199,** 137–147 (1988).
25. Frank, J. *et al.* SPIDER and WEB: processing and visualization of images in 3D electron microscopy and related fields. *J. Struct. Biol.* **116,** 190–199 (1996).
26. Schuwirth, B. S. *et al.* Structures of the bacterial ribosome at 3.5 Å resolution. *Science* **310,** 827–834 (2005).
27. Wriggers, W., Milligan, R. A. & McCammon, J. A. Situs: A package for docking crystal structures into low-resolution maps from electron microscopy. *J. Struct. Biol.* **125,** 185–195 (1999).
28. Jones, T. A., Zhou, J. Y., Cowan, S. W. & Kjeldgaard, M. Improved methods for building protein models in electron density maps and the location of errors in these models. *Acta Crystallogr. A* **A47,** 110–119 (1991).
29. Pettersen, E. F. *et al.* UCSF Chimera—a visualization system for exploratory research and analysis. *J. Comput. Chem.* **25,** 1605–1612 (2004).

Supplementary Information is linked to the online version of the paper at www.nature.com/nature.

Acknowledgements This work was supported by grants from the VolkswagenStiftung and the Deutsche Forschungsgemeinschaft SFB594 (to R.B.) and SFB638 (to I.S.) and by the European Union and Senatsverwaltung für Wissenschaft, Forschung und Kultur Berlin (UltraStructureNetwork).

Author Information Coordinates of the atomic models of SRP have been deposited in the PDB under accession numbers 2j28 and 2j37. The cryo-electron microscopic maps have been deposited in the 3D-EM database under accession numbers EMD1261 (*E. coli* SRP–RNC), EMD1263 (*E. coli* RNC) and EMD1264 (mammalian SRP-RNC). Reprints and permissions information is available at www.nature.com/reprints. The authors declare no competing financial interests. Correspondence and requests for materials should be addressed to R.B. (beckmann@lmb.uni-muenchen.de).